

Camera Raw Image Processing and Registration Using Raw CFA Images

K. Murugesha^a, Mahesh P K^b

^a Assistant Professor, Dept. of ECE, MVJ College of Engineering, Bangalore, India,

^b Professor and Head, Dept. of ECE, ATME College of Engineering, Mysore, India.

^a muru.global@gmail.com, ^b mahesh.k.devalapur@gmail.com

Article History: Received: 10 January 2021; Revised: 12 February 2021; Accepted: 27 March 2021; Published online: 28 April 2021

Abstract: Abstract— RAW — a multimedia file with image details collected by the camera concerning the pixel values of the sensor and the text information. The processing of RAW is important ignoring the replication of images, to save space, to encourage the operation of image files and to have continuous capture. The RAW is emphasized as a digital adverse and varies according to the scale depending on the manufacturer of the hardware. The proposed workflow is to Extract and process RAW sensor information from the RAW files and view the picture format details. Image quality is the significant parametric quantity that defines the captured RAW image. With no built-in compression (RAW) the most extreme resolution brings about picture from any advanced camera. The MATLAB R2016a was used to execute the purpose of the workflow and the analysis. We examined direct registration of raw images based on an imaging model, which shows precise estimation of motion among severely aliased raw images. The proposed method is verified through experiments using synthetic and real images.

1. Introduction

In the fields of image processing and computer vision, researchers often are unaware of the origins of the images they study. We only design algorithms for multivariable functions, stochastic fields, and connected pixels graphs (usually an 8-bit strength or three-channel RGB image with an 8-bits channel).

However, it is sometimes necessary to link an image to the light of the scene from which it was taken. This is true, for instance, for processes that simulate behavior, such as some HDR techniques and scientific imagery (e.g., astronomy). In this situation, it is important to understand the entire processing chain that occurred after the image was captured. If possible, the best image to discuss is the sensor information straight from the camera, the raw images.

Raw data access is also useful for those who wish to concentrate on the image processing steps necessary to convert data from the camera sensor to a usable output image. For example, a researcher working on Bayer pattern images demo algorithms would need access to those data for actual testing.

While some sensors produce only a compressed digital image, some cameras provide direct access to the image sensor's data. These DSLRs (Digital single lens reflex cameras) are usually in the mid- to high-price range and have the ability to export RAW data files. In the future, sensor data from other types of cameras (such as cell phones) will be accessed, at which point the following rules may also apply (although the basic programming might be different).

'RAW' is a term that refers to a group of computer files that typically contain an uncompressed image that contains the sensor pixel values as well as various meta-information about the camera image (the Exifdata). A sizable portion of RAW files are created in proprietary file formats (.NEF Nikons, Canon's.CR2, etc.) and at least one common .DNG file format that represents the Digital Negative. The preceding demonstrates how digital photographers can view these files as master originals, records of all the scene information they collect. RAW files are intentionally opaque data structures that have been effectively reverse engineered [1] to allow access to the raw data contained within. The remainder of these bits use the capitalized term RAW to refer to an Image file in one or more file formats (e.g., CR2), while unprocessed Pixel Values are directly outputs from a camera's image sensor as a (lowercase) raw image.

While the raw data from an image sensor clearly provides details about the scene, the human eye is typically unidentifiable. As illustrated in Figure 1, it is a single-channel picture of channel intensity with a possible non-zero minimum value for 'black' that contains integer values containing 10-14 bits of data. No color in an image will exceed a saturation point determined by the physical pixel CCD, rather than an intrinsic 'white' value. Additionally, the display can be larger than the sensor's intended pixel dimensions, including an unexposed left and beyond pixel boundary.

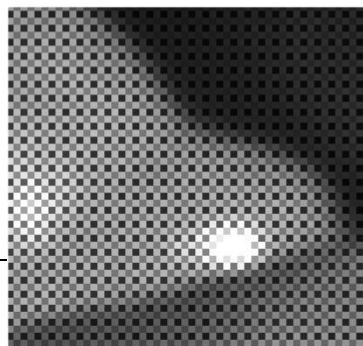


Figure 1: Detail of raw sensor data image.

Typically, a Color Filter Array is a row sensor result (CFA). This is an m -by- n pixel array (m and n are the sensor dimensions) that contains information about a single color channel: red, green, or blue. Only a scalar value can be saved if light on a particular photo sensor is recorded as a certain number of electrons in a condenser; the three-dimensional life of observative light cannot be preserved by a single pixel.

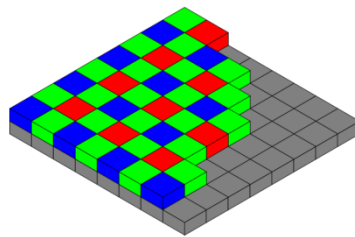


Figure 2: CFA layout by Bayer. Each pixel reflects, depending on the structure inside the table, the red, blue, or green value of the light incident in the sensor. Demosaicing can be extended to get all three elements at each venue.

The RAW Image Editing Workflow

The above mentioned existence of the raw data must be taken into consideration in order to work with and view images in the MATLAB from sensor data. In the first order, the workflow represented in Figure 3 illustrates how a "correct" displayable output image can be taken from the raw sensor data.

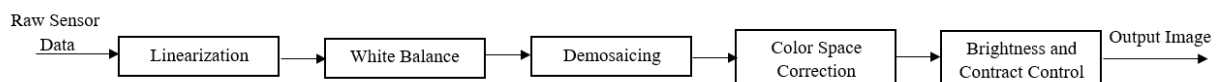


Figure 3: Proposed workflow for raw image processing.

The human eye is incapable of recognizing raw data acquired by an imaging sensor. The pipeline for digital camera processing refers to a series of algorithms that transform the sensor data collected into images that faithfully reproduce the scene seen by the photographer. Typically, a spatial multiplexing sensor is a color filter array consisting of red, green, and blue filters spread across the monitor. Defeat pixel removal and demonstration, color change, gamma correction, and noise reduction are all products of the image sensor's data set. After the optical pipeline recovers the color signal, the rendered image is compressed using an image compression algorithm.

Cameras acquire raw (or minimally processed) files. converts the incident light to an intensity, which is then produced in the CCD or CMOS channel and finally quantized to produce a voltage value [2]. Typically, a factor of 4096 or 16384 values are used for quantization. It is not compressed into an 8-bit format (256 values). The outcome of an inexperienced imaging pipeline several techniques have been used, including demasking, denoising, deblurring, and quantizing.

Numerous multi-image algorithms are fed a series of preprocessed images, which results in artifacts, as a result, methodologies are better equipped to deal with difficult images [3, 4, 5, 6, 7, 8]. It refers to the process of de-mosaicing, denoising, and potentially super-resolving images. In general, image processing methods can be classified into two categories: registration, in which images are represented using common coordinates, and combination, in which data is used to form an image. We showed that there was no practical or efficient registration mechanism and proposed a two-step approach that was both efficient and effective. Assuming the

images register correctly, a large number of high-quality images must be produced at a high computational and memory cost.

2. Preprocessing of RAW images

Let $(I_{RAW}^j)_{1 \leq j \leq N_{im}}$ denote a series of images beginning with the RAW images of N_{im} . This is how our image-formation algorithm structures the sequence of images $(I_{RAW}^j)_{1 \leq j \leq N_{im}}$. To begin, the images are transformed using an additive, white, and homoscedastic noise variance transform to approximate homoscedastic, white, or Gaussian-distributed white noise. The photos' histograms are then resized. The objective is to streamline the registration and configuration processes.

2.1.1 Color Handling

We begin with essential techniques and instructions for working with color channels. Relationship between channels Allow for a red-colored picture. I have three indices: c_1 , c_2 , and c_3 . In the channel, the strength value at location (k, l) is denoted by the symbol $I_{k,l,c}$.

Aspect ratio of the reference image and the input channel informally, consider I_{RAW} to be an image. In this chapter, we will use the classical Bayer's default color filter set [9]. The intensity value (k, l) is equal to (or equal to) the channel's parameter at (or known as)

$$c = k \% 2 + l \% 2 + 1$$

$$n \% 2 = \begin{cases} 0 & \text{if } n \text{ is even,} \\ 1 & \text{if } n \text{ is odd.} \end{cases}$$

2.2.2 Variance Stabilizing Transform

Gaussian, additive, and homogeneous phases of validation and composition. However, randomness occurs in RAW images as a result of Poisson noise produced by photon emission, as well as thermal and electronic noise [2, 10, 11]. The variation of additive, white Gaussian, and signal-dependent noise must be approximately equal to the signal.

Variance stabilizing transform.

A variance-smoothing transform (VST) must be used to stabilize the signal-dependent noise [10, 12]. To implement a VST on an image, I is chosen pixel by pixel to ensure that the noise in $f(I)$ is constant. The distribution of f is determined by the noise parameter g , and their relationship is defined by the function $g: R \rightarrow R^+$, which has an inverse variance relationship (in D). [12] Demonstrates that an appropriate response to the issue of whether or not to select

$$f(u) \propto \int_0^u \frac{ds}{\sqrt{g(s)}}$$

Anscombe transform. The variance of the noise, i.e., $g(u) = au + b$, can be referred

$$f(u) \propto \sqrt{au + b}$$

The generalized Anscombe transform was first designed for Poisson noise.

Utilization of the VST We use the VST for the sequence $(I_{RAW}^j)_{1 \leq j \leq N_{im}}$. To begin, the noise contribution in the first RAW image was calculated using the Ponomarenko et al method's. The coefficients a_c and b_c are both computed by linear least squares. Finally, for each image, I_{CFA}^j is found to be

$$(I_{CFA}^j)_{k,l} = \sqrt{a_c (I_{RAW}^j)_{k,l} + b_c}$$

where $c = k \% 2 + l \% 2 + 1$

The results are non-inverted at the output of the Design Patterns sub-algorithm. Notice that to avoid misuse the VST is not to just use the inverse. As a hypothesis, inversed VST can be formed in [13].

2.3 Image Formation from RAW images

We propose a method for quickly and efficiently generating images from RAW images in this section. This is an alternative to our image fusion procedure.

2.3.1 Proposed Algorithm

Given a series $(I_{RAW})_{1 \leq j \leq N_{im}}$ of N_{im} with scale $s > 0$, a color image scale has $\sigma_s > 0$ coefficients as illustrated in Figure 4. In this case, the first example is randomly chosen as the reference example.

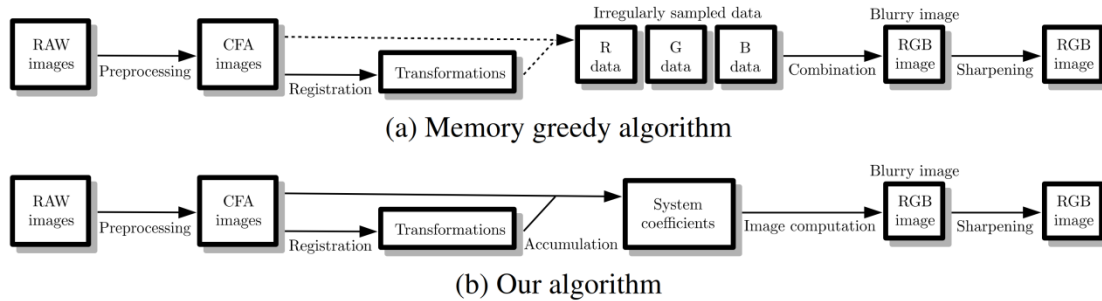


Figure 4: The basic processes for image formation but (a) and (b) are considered identical as is with the accumulation step, the images are sequentially processed, the combination of the irregularly sampled data is replaced by the algorithm.

Removing steps that could not be executed prior to shaping the final product In algorithm 5.2, the sequence $(I_{CFA})_{1 \leq j \leq N_{im}}$ is the product of preprocessing is given as the first $(I_{jRAW})_{1 \leq j \leq N_{im}}$.

Registration. The transition's transformation is set to the personality. The homographic transformation ϕ between I_{CFA} and I_{CFA} , which is calculated using a two-step process.

Accumulation. This is mostly the same, except that the images to be counted are mosaicked. $2x$ -image demosaicing is a form of supersampling We use this formula: Thus, as suggested, we use $NKR = 2$. The coefficients in the outputs in the range $(x_0, c) \in \Omega[\lambda M], [\lambda N] \times \{1, 2, 3\}$ for each output pixel (x_0, c) are accumulated.

In the second step, the CFA images were analyzed sequentially. For each pixel $(k, l) \in \Omega_{M, N}$, the channel c is computed, and the corresponding pixel in the zoomed reference system is computed.

Image computation. For each output pixel, the strength $A_{x_0, c}$ and $b_{x_0, c}$ are obtained. When formed, the image defines of size $\lambda M \times \lambda N$, which is blurred.

Sharpening. To remove the motion filtering blur, we use the DCT (decomposition with a transform) to DCT the image.

2.4 Experiments

We assess the true output on real data with the image formation algorithm that was introduced in this section. Two sequences of RAW images are of equivalent in quality. The instructions on conducting the typical experiment where the spatial repartition of the samples is not uniform, the limits of our approach are seen in the second section of this example. On the contrary, which has a uniform sample repartition Recall that the procedure was carried out on synthetic data in order to be tested in the previous chapter. The combination method was employed in order to increase the computational efficiency of the classical kernel method.

2.4.1 Experimental Setup

The image is considered to be of a static outdoor scene, each consisting of 201 separate RAW images. Each of the images was captured using the Olympus E-M5 II, which was set to sequential shooting. But the camera was set on a tripod with the stabilization switch off. Thus, minor camera adjustments were permitted, as well as super-resolution. The images of a series are impacted by motion of the camera, quantization (14-bit), and probably minor variations in illumination.

In both cases, we only hold the central 512×512 element, which is free of distortion. The preceding image (or one of the initial images) acts as the reference image for preprocessing and registration, but not for combination. Uniformly applying is used on the images that remain (N_{im} is set to approximately 200). We checked $\lambda = 1.5$ and ordinary double demosaicing (using just $2x$ interpolation) (demosaicking and super-resolution). We apply to red and blue zooms with respect to factor 2.

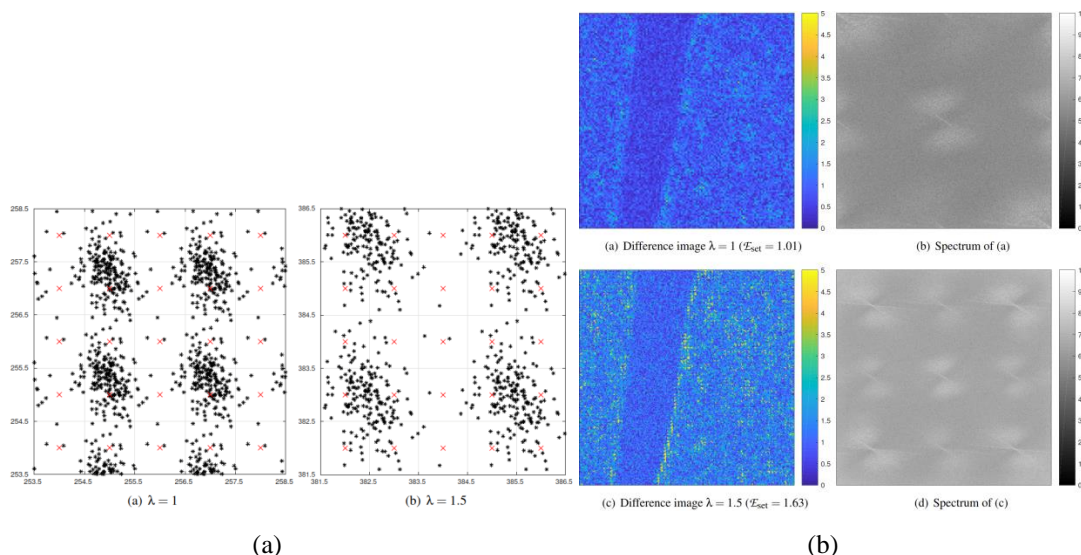


Figure 5: (a) The spatial repartition of the irregularly sampled data, (b) The comparison between two individual images from a single sequence

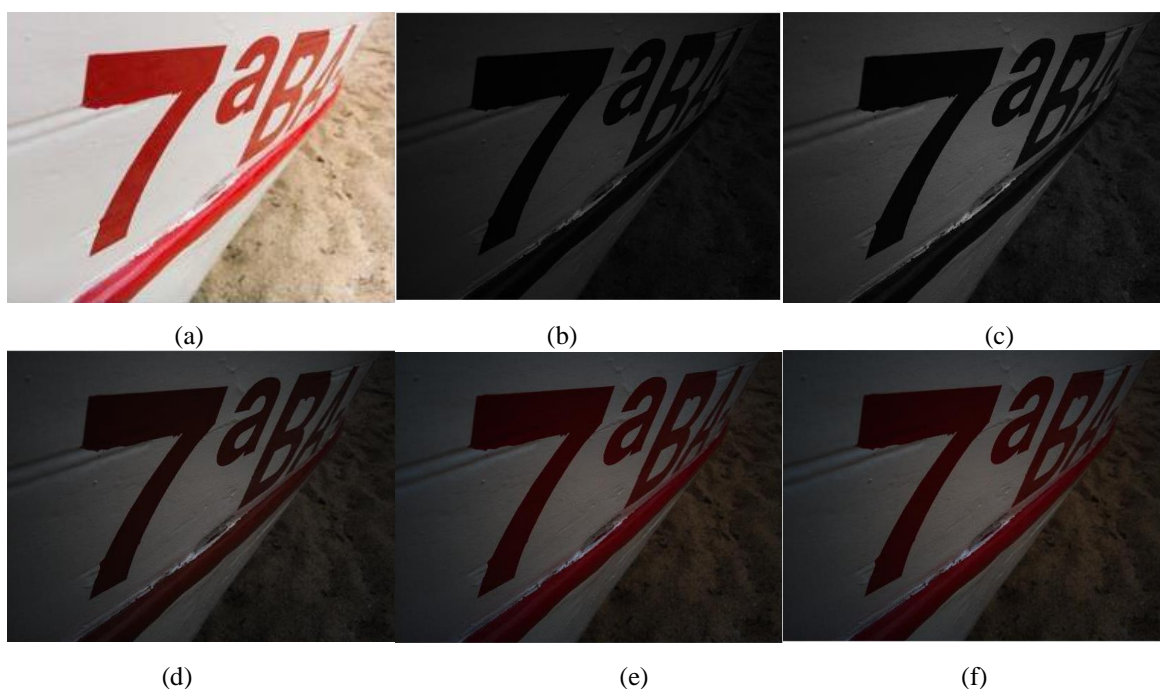


Figure. 6 (a) RAW Image, (b) Linearized RAW Image, (c) White Balanced Image (d) Demosaicised Image, (e) Brightness & Gamma Correction, (f) Color Space Conversion

3. Conclusion:

Here, we suggest an image forming process that was presented. Formal preprocessing involves setting the noise curve and optimizing the histograms. The two-step registration technique, which was illustrated, is then applied to the mosaicked images. The image processing techniques are divided into processing, where the images are taken one at a time, and estimation, where the images are collected. The classical "blur" introduced by the kernel is turned into a sharpening method, with blur getting more intense as you get close to the output of the kernel.

References

1. R. Abergel and L. Moisan. "The Shannon Total Variation". In: Journal of Mathematical Imaging and Vision (2017), pp. 1–30. ISSN: 1573-7683. DOI: 10.1007/s10851-017-0733-5(see pp. 18, 38, 58, 62, 64, 134, 142, 146).

2. C. Aguerrebere, J. Delon, Y. Gousseau, and P. Muse. "Study of the digital camera acquisition process and statistical modeling of the sensor raw data". In: (2013). URL: <https://hal.archives-ouvertes.fr/hal-00733538>(see pp. 258, 259).
3. S. Farsiu, D. Robinson, M. Elad, and P. Milanfar. "Advances and challenges in super-resolution". In: *International Journal of Imaging Systems and Technology* 14.2 (2004), pp. 47–57. ISSN: 1098-1098. DOI: 10.1002/ima.20007(see pp. 15, 35, 188, 258).
4. S. Farsiu, D. Robinson, M. Elad, and P. Milanfar. "Dynamic demosaicing and color superresolution of video sequences". In: *Image Reconstruction from Incomplete Data III*. Vol. 5562. International Society for Optics and Photonics. 2004, pp. 169–179. URL: <http://citeseerx.ist.psu.edu/viewdoc/download?doi=10.1.1.102.8268&rep=rep1&type=pdf>(see pp. 15, 35, 188, 258).
5. T. Gotoh and M. Okutomi. "Direct super-resolution and registration using raw CFA images". In: *Computer Vision and Pattern Recognition, 2004. CVPR 2004. Proceedings of the 2004 IEEE Computer Society Conference on*. Vol. 2. IEEE, pp. II–II. DOI: 10.1109/CVPR.2004.1315219(see pp. 15, 16, 35, 188, 258).
6. W. C. Kao. "High Dynamic Range Imaging by Fusing Multiple Raw Images and Tone Reproduction". In: *IEEE Transactions on Consumer Electronics* 54.1 (2008), pp. 10–15. ISSN: 0098-3063. DOI: 10.1109/TCE.2008.4470017(see pp. 15, 35, 188, 258).
7. S. Farsiu, M. Elad, and P. Milanfar. "Multiframedemosaicing and super-resolution of color images". In: *IEEE transactions on image processing* 15.1 (2006), pp. 141–159. DOI: 10.1109/TIP.2005.860336(see pp. 15, 16, 35, 188, 258).
8. P. Vandewalle, K. Krichane, D. Alleysson, and S. Stüsstrunk. "Joint demosaicing and super-resolution imaging from a set of unregistered aliased images". In: *Electronic Imaging 2007*. International Society for Optics and Photonics. 2007, 65020A–65020A. DOI: 10.1117/12.703980(see pp. 15, 16, 35, 188, 191, 258).
9. T. Briand. "Low Memory Image Reconstruction Algorithm from RAW Images". In: *2018 IEEE 13th Image, Video, and Multidimensional Signal Processing Workshop (IVMSP)*. 2018, pp. 1–5. DOI: 10.1109/IVMSPW.2018.8448561(see pp. 30, 50, 257, 258).
10. M. Colom, A. Buades, and J-M Morel. "Nonparametric noise estimation method for raw images". In: *JOSA A* 31.4 (2014), pp. 863–871. DOI: 10.1364/JOSAA.31.000863 (see p. 259).
11. Foi, M. Trimeche, V. Katkovnik, and K. Egiazarian. "Practical Poissonian-Gaussian noise modeling and fitting for single-image raw-data". In: *IEEE Transactions on Image Processing* 17.10 (2008), pp. 1737–1754. DOI: 10.1109/TIP.2008.2001399 (see p. 259).
12. M. Lebrun, M. Colom, A. Buades, and J-M Morel. "Secrets of image denoising cuisine". In: *Acta Numerica* 21 (2012), pp. 475–576. DOI: 10.1017/S0962492912000062 (see p. 259).
13. M. Makitalo and A. Foi. "A Closed-Form Approximation of the Exact Unbiased Inverse of the Anscombe Variance-Stabilizing Transformation". In: *IEEE Transactions on Image Processing* 20.9 (2011), pp. 2697–2698. ISSN: 1057-7149. DOI: 10.1109/TIP.2011.2121085(see p. 259)..